Phase Dependent Current Statistics in a Short-Arm Andreev Interferometer

E.V. Bezuglyi[1,3], E.N. Bratus[1], V.S. Shumeiko[2], and V.M. Vinokur[3]

[1] Institute for Low Temperature Physics and Engineering, Kharkov 61103, Ukraine
[2] Chalmers University of Technology, Gothenburg S-41296, Swedeneugene@fy.chalmers.se
[3] Materials Science Division, Argonne National Laboratory, Argonne IL 60439, USA

Summary. We calculate analytically the full counting statistics for a short normally conducting diffusive wire connecting a normal reservoir and a short superconductor-normal metal-superconductor junction, at arbitrary applied voltages and temperatures. The cumulant-generating function oscillates with the phase difference ϕ across the junction and approaches the normal-state value at $\phi = \pi$. At $T = 0$ and at applied voltage much smaller than the proximity gap Δ_ϕ, the current noise P_I doubles and the third current cumulant C_3 is 4 times larger compared to the normal state; at $eV \gg \Delta_\phi$ they acquire large excess components. At the gap edge, $eV = \Delta_\phi$, the differential shot noise dP_I/dV exhibits sharp peak, while the differential Fano factor dP_I/dI turns to zero along with the differential resistance, which reflects the transmission resonance associated with the singularity of the density of states. At nonzero temperature, C_3 shows a non-monotonous voltage dependence with a dip near $eV = \Delta_\phi$; the zero-bias slope of $C_3(V)$ is much larger (up to 5 times) than at the zero temperature.

During last few years the statistics of quantum and thermal fluctuations of the electric current in mesoscopic systems has been attracted a rapidly growing attention. It was recognized that measuring the fluctuation properties of mesoscopic conductors provide unique and important information about correlations and statistics of charge carriers, the information that is not accessible through conventional conductance measurements. An adequate and powerful theoretical approach to the fluctuations was built on the concept of full counting statistics (FCS), i.e., the statistics of the number of particles transferred through the conductor. The concept of FCS, which appeared first in quantum optics, was extended to normal electron systems [1] and then successfully applied to superconducting structures [2].

A. Glatz et al. (eds.), Theory of Quantum Transport in Metallic and Hybrid Nanostructures 241–255.

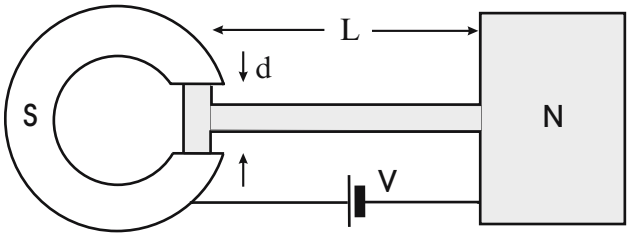

Fig. 1. A model of Andreev interferometer. A diffusive wire of the length L connects a normal reservoir (N) and short SNS junction of the length d; magnetic flux Φ threads a superconducting loop (S) of the interferometer.

The basic problem of the FCS is to calculate a probability $P_{t_0}(N)$ for N particles to pass a system during an observation time t_0. Equivalently, one can find a cumulant generating function (CGF) $S(\chi)$,

$$\exp[-S(\chi)] = \sum\nolimits_N P_{t_0}(N) \exp(iN\chi), \tag{1}$$

which determines the current correlation functions as follows:

$$C_n \equiv \frac{1}{e^n} \int_0^{t_0} dt_1 \ldots \int_0^{t_0} dt_n \langle\langle \hat{I}(t_1) \ldots \hat{I}(t_n) \rangle\rangle = - \left(\partial / i\partial\chi\right)^n S(\chi)|_{\chi=0}\,, \tag{2}$$

where $\langle\langle \ldots \rangle\rangle$ denotes the irreducible part (cumulant) of a correlation function. The first two cumulants, $C_1 = \overline{N} \equiv \sum_N N P_{t_0}(N)$ and $C_2 = \overline{(N - \overline{N})^2}$, correspond to the average current $I = (e/t_0)C_1$ and noise power $P_I = (2e^2/t_0)C_2$. Intense studies of the current noise have led to a number of interesting results concerning statistical correlations in the current transport (for a review, see Ref. [3]), and the effective charge q_{eff} transferred during an elementary transport event. The third cumulant $C_3 = \overline{(N - \overline{N})^3}$ has recently attracted a special interest as the lowest-order correlation function which is not disguised by equilibrium fluctuations [4]. First measurements of $C_3(V)$ in the tunnel junction [5] have revealed a high sensitivity of this cumulant to an electromagnetic environment [6].

In normal metal (N)/superconducting (S) hybrid structures, the basic mechanism of charge transport at subgap energies, $E < \Delta$, is due to Andreev reflection of quasiparticles at the NS boundary [7], i.e., conversion of electrons incident from the normal side of the junction to retroreflected holes, accompanied by escape of Cooper pairs into the superconductor. During an elementary Andreev reflection event, the effective charge transferred through the NS interface is twice the electron charge, $q_{eff} = 2e$. This charge doubling strongly affects the current statistics in the NS junctions. For example, it leads to a factor of two increase in the magnitude of a zero-bias shot noise in the NS junctions as compared to that in normal ones [2, 8]. At finite biases, the effective charge becomes dependent on the applied voltage [9, 10], due to variations of the size of the proximity region near the NS boundary, where the quantum coherence holds between the electrons and retroreflected holes.

In the Andreev interferometers (see Fig. 1), the phase relations between the electron and hole wavefunctions in the normal wire can be controlled by the magnetic flux enclosed by a superconducting loop, which results in the periodic dependence of transport characteristics of the interferometer on the superconducting phase difference ϕ across the SNS junction. Initially, the oscillations of the conductance were investigated both experimentally (see a review in Ref. [11]) and theoretically [12], and, more recently, the oscillations in the current noise were reported [10].

Motivated by the growing interest in high-order correlation functions, we develop in the present Paper a systematic approach to full statistics of charge transport in Andreev interferometers. We adopt several simplifying assumptions, which enables us to present an analytical solution for the CGF and, without a loss of generality, to clearly demonstrate essential features of coherent effects in the current statistics in NS structures. Our approach is based on the extended Keldysh-Green technique [13, 14], in which the CGF is determined by the equation

$$(-ie/t_0)\partial S/\partial\chi = I(\chi), \;\; I(\chi) = \frac{1}{8e}\int dE \mathrm{Tr}\check{\tau}_K\check{I}, \quad \check{\tau}_K = \sigma_z\tau_x. \tag{3}$$

The Pauli matrices σ (τ) operate in the Nambu (Keldysh) space. The counting current $I(\chi)$ is to be found from the quantum kinetic equations [15] for the 4×4 matrix Keldysh-Green function $\check{G}$ in the mesoscopic normal region of the interferometer confined between the reservoirs,

$$\sigma_N\left[\sigma_z E, \check{G}\right] = i\hbar\mathcal{D}\partial\check{I}, \quad \check{I} = \sigma_N\check{G}\partial\check{G}, \quad \check{G}^2 = \check{1}, \tag{4}$$

where $\mathcal{D}$ is the diffusion coefficient, ∂ denotes spatial derivative, and σ_N is the normal conductivity per unit length. The counting field χ is introduced via a modified boundary condition involving the gauge transformation of the local-equilibrium function $\check{G}_R$, e.g., in the right (R) normal reservoir,

$$\check{G}_R(\chi) = \exp(i\chi\check{\tau}_K/2)\check{G}_R\exp(-i\chi\check{\tau}_K/2). \tag{5}$$

A brief overview of this technique in the particular case of normal structures is given in the Appendix.

For a multi-terminal structure of Fig. 1, the solution of Eq. (4) has to be found separately in each arm of the interferometer, taking into account the matching condition following from the Kirchhoff's rule for partial counting currents at the node [16]. The problem simplifies if the junction length d is much smaller than the length L of the interferometer wire (or, more precisely, in the case where the wire resistance dominates the net interferometer resistance). In this case, the wire weakly affects the spectrum of the junction [17], which thus can be considered as an effective left (L) reservoir. Correspondingly, the function $\check{G}_L$ which imposes the boundary condition to Eq. (4) at the junction node, is to be constructed from the Green and distribution functions taken at the middle of a closed equilibrium SNS junction.

Furthermore, if d is much smaller than the coherence length $\xi_0 = \sqrt{\hbar\mathcal{D}/\Delta}$, these Green functions take the BCS form, with the phase-dependent proximity gap $\Delta_\phi = \Delta|\cos(\phi/2)|$ [18]. This results in the BCS-like singularity at the gap edge in the density of states (DOS) of the normal wire and suppression of the DOS at $E < \Delta_\phi$. Within such model, the problem of current statistics in the Andreev interferometer reduces to the calculation of the CGF for an NS junction with the effective order parameter Δ_ϕ in the superconducting reservoir.

Proceeding with this calculation, we encounter a common technical difficulty, namely, the violation of the standard triangle form of $\check{G}$ in the Keldysh space which results from the gauge transformation in Eq. (5). In such a situation, Eq. (4) cannot be decomposed into the Usadel equation for the Green's functions and the kinetic equations for the distribution functions, and therefore the well developed methods for solving Keldysh-Green's equations quite cannot be applied. This is the reason why the FCS problem in the NS structures requires generally a numerical analysis of the whole 4×4 matrix boundary problem; such an analysis has been carried out so far only in the limit of small characteristic energies $\{eV, T\} \ll \Delta$ [9, 10].

In some particular cases, however, the analytical solution to this problem can be attained by the methods of the generalized circuit theory [19, 20]. Within this approach, the CGF for a mesoscopic connector between two reservoirs is expressed in terms of the distribution $\rho(\mathrm{T})$ of the transparencies of the conduction channels,

$$S(\chi) = \frac{gt_0}{4e^2}\int dE \int_0^1 d\mathrm{T}\rho(\mathrm{T})\mathrm{Tr}\ln\check{W}(E,\mathrm{T},\chi), \tag{6}$$

$$\check{W} = 1 + (\mathrm{T}/4)(\{\check{G}_L, \check{G}_R(\chi)\} - 2), \tag{7}$$

where g is the connector conductivity. Eq. (6) generally applies to the normally conducting structures with arbitrary $\rho(\mathrm{T})$. It was also applied to the superconducting tunnel junctions [21] and point contacts [20, 22] with a singular transparency distribution localized at the junction transparency. In general NS structures, the statistics of conducting modes, in contrast to their behavior in normal structures [23, 24], do not reduce to statistics of transparencies - due to dephasing between the electron and hole wavefunctions described by the left-hand side (lhs) of Eq. (4) - but requires the knowledge of full scattering matrices. However, if the characteristic energies are much smaller than the Thouless energy, $\{eV, T\} \ll E_{Th} = \hbar\mathcal{D}/L^2$, the dephasing term in Eq. (4) can be neglected, and the transparency statistics for a normal wire [23] can be applied to the NS structure. In long junctions, $L \gg \xi_0$, where the Thouless energy is small, $E_{Th} \ll \Delta$, the quasiparticle spectrum is structureless at small energies, $E \ll E_{Th}$, which results in linear voltage dependence of the CGF and, correspondingly, of all cumulants at $eV \ll E_{Th}$ [14]. In the opposite limit, $eV \gg E_{Th}$, the CGF for a long junction can be found within the so-called "incoherent" approximation [25], by neglecting the contribution of

the coherent proximity region. The calculations in Refs. [14] and [25] lead to the conclusion that the FCS exhibits the reentrance effect: In both limits, $eV \ll E_{\rm Th}$ and $eV \gg E_{\rm Th}$, it is described by the same expression for $S(\chi)$. An interesting situation occurs in NS junctions with opaque interfaces dominating the net resistance [26]. In this case, the crossover between the coherent and incoherent transport regimes occurs at very small voltage of the order of the inverse dwell time of quasiparticles confined between the interface barriers.

In our work we focus on short NS junctions with the length smaller than ξ_0 and, correspondingly, with large Thouless energy, $E_{Th} \gg \Delta_\phi$. In such situation, the energy region of negligibly small dephasing, $E \ll E_{Th}$, overlaps with the region $E \gg \Delta_\phi$, in which the NS junction behaves as the normal system. This enables us to apply Eq. (6) and the transparency statistics for diffusive normal conductor at arbitrary voltages and temperatures, and obtain the analytical solution of the FCS problem in the full range of V and T.

The calculation of the integrand in Eq. (6) is performed as follows. The Keldysh-Green function $G_R(\chi)$ in the normal reservoir is traceless in the Keldysh space and therefore it can be expanded over the Pauli matrices τ as

$$\check{G}_R(\chi) = \boldsymbol{\tau}(\boldsymbol{g}_1 + \sigma_z \boldsymbol{g}_z), \quad \boldsymbol{g}_1 \boldsymbol{g}_z = 0, \quad \boldsymbol{g}_1^2 + \boldsymbol{g}_z^2 = 1, \quad \boldsymbol{\tau} = (\tau_x, \tau_y, \tau_z), \tag{8}$$

where the vectors $\boldsymbol{g}_{1,z}(\chi)$ are expressed through the local-equilibrium distribution functions in the voltage biased electrode. In the subgap energy region, $E < \Delta_\phi$, the function $\check{G}_L$ at the junction node is the unity matrix in the Keldysh space proportional to the Nambu matrix Green's function $\hat{g}$,

$$\check{G}_L = \hat{g} = \sigma_y \exp(\sigma_x \theta_\phi), \quad \hat{g}^2 = 1, \quad \theta_\phi = \operatorname{arctanh}(E/\Delta_\phi). \tag{9}$$

Then the calculation of the trace in the Nambu space in Eq. (7) is reduced to the summation over the eigenvalues $\sigma = \pm 1$ of the matrix $\hat{g}$,

$$\operatorname{Tr} \ln \check{W} = \sum\nolimits_\sigma \operatorname{Tr}_\tau \ln \check{W}_\sigma, \quad \check{W}_\sigma = a + \boldsymbol{\tau}\boldsymbol{b}, \tag{10}$$

$$a = 1 - \mathrm{T}/2, \quad \boldsymbol{b} = (\mathrm{T}/2)(\sigma \boldsymbol{g}_1 - i \boldsymbol{g}_z \sinh \theta_\phi). \tag{11}$$

Noticing that any 2×2 matrix can be presented in exponential form as

$$\check{W}_\sigma = \exp(\ln w + \varphi \check{p}), \tag{12}$$

$$w^2 = a^2 - \boldsymbol{b}^2, \quad \cosh \varphi = a/w, \quad \check{p} = \boldsymbol{\tau}\boldsymbol{b}/w \sinh \varphi, \quad \operatorname{Tr} \check{p} = 0, \tag{13}$$

where w is independent of σ due to orthogonality of the vectors $\boldsymbol{g}_1$ and $\boldsymbol{g}_z$, one easily obtains $\operatorname{Tr}_\tau \ln \check{W}_\sigma = \ln w^2$ and $\operatorname{Tr} \ln \check{W} = 2 \ln w^2$. At $E > \Delta_\phi$, the function G_L is traceless in the Keldysh space,

$$\check{G}_L = \hat{g}(\boldsymbol{\tau}\boldsymbol{g}_L), \quad \hat{g} = \sigma_z \exp(\sigma_x \theta_\phi), \quad \theta_\phi = \operatorname{arctanh}(\Delta_\phi/E), \tag{14}$$

where the vector $\boldsymbol{g}_L$ is constructed from the equilibrium distribution function at zero potential. In this case, the 4×4 matrix $\check{W}$ has the form $\check{W} = a + \boldsymbol{\sigma}\boldsymbol{b}$, where a and $\boldsymbol{b}^2$ are scalars,

$$a = 1 - (\mathrm{T}/2)(1 - \boldsymbol{g}_L \boldsymbol{g}_{\boldsymbol{z}} \cosh\theta_\phi), \tag{15}$$

$$\boldsymbol{b}^2 = (\mathrm{T}/2)^2[(\boldsymbol{g}_L \boldsymbol{g}_{\boldsymbol{1}})^2 - (\boldsymbol{g}_L \times \boldsymbol{g}_{\boldsymbol{z}})^2 \sinh^2\theta_\phi], \tag{16}$$

therefore it can also be transformed to the exponent form similar to Eqs. (12) and (13), with the traceless matrix $\check{p} = \boldsymbol{\sigma b}/w \sinh\varphi$. Following this line, we obtain $\mathrm{Tr}\ln\check{W} = 2\ln w^2$, and then, integrating over T in Eq. (6), we arrive at the final expressions for the CGF

$$S(\chi) = \frac{gt_0}{4e^2}\int_0^\infty dE\, S(E,\chi), \quad S(E,\chi) = \begin{cases} 2\theta^2, & E < \Delta_\phi, \\ \theta_+^2 + \theta_-^2, & E > \Delta_\phi, \end{cases} \tag{17}$$

where the quantities θ and $\theta_\pm$ are given by explicit relations,

$$Z(0)\cosh^2\theta = Z(2\chi)\cosh^2\theta_\phi, \tag{18}$$

$$Z(0)\cosh\theta_\pm = [Z(\chi) + \cos\chi - 1]\cosh\theta_\phi \pm \tanh\frac{\epsilon}{2}\,[\sinh p - \sinh(p - i\chi) - i\sin\chi]\Big(1 - \frac{\cosh\epsilon + 1}{\cosh p - 1}\sinh^2\theta_\phi\Big)^{1/2}, \tag{19}$$

$$\theta_\phi = \mathrm{arctanh}\left[(\Delta_\phi/E)^{\mathrm{sgn}(E-\Delta_\phi)}\right], \tag{20}$$

$$Z(\chi) = \cosh(\epsilon) + \cosh(p - i\chi), \quad \epsilon = E/T, \quad p = eV/T. \tag{21}$$

By using Eqs. (2) and (17)-(21), one can obtain analytical expressions for all cumulants. At zero temperature, the calculation essentially simplifies. Indeed, at $T \to 0$ and $E > eV$, the dominating terms in Eqs. (18)-(21) are proportional to $\exp(\epsilon)$, and therefore θ and $\theta_\pm$ are equal to θ_ϕ. This implies that the CGF is independent of the counting field at these energies, and all cumulants turn to zero. At $E < eV$, the terms with $\exp(p - in\chi)$ dominate, and we arrive at simple relations,

$$\cosh\theta = e^{-i\chi}\cosh\theta_\phi, \quad \cosh\theta_\pm = e^{-i\chi}\cosh\theta_\phi \pm (e^{-i\chi} - 1). \tag{22}$$

At subgap voltage, $eV < \Delta_\phi$, when the charge transport at $T = 0$ is only due to the Andreev reflection, the current I, the shot noise power P_I, and the third cumulant C_3 read

$$I = I_\Delta q(z), \quad q(z) = \int_0^z \frac{dx}{x}\mathrm{arctanh}x, \quad P_I = 2e\big[I - I_\Delta f(z^{-1})\big], \tag{23}$$

$$C_3 = \overline{N} - \frac{\overline{N}_\Delta}{2z^2}\left[(5z^2 - 3)f(z^{-1}) + z\right], \quad I_\Delta = \frac{g\Delta_\phi}{e}, \quad \overline{N}_\Delta = \frac{I_\Delta t_0}{e}, \tag{24}$$

$$f(z) = (1/2)[z - (z^2 - 1)\mathrm{arctanh}z^{-1}], \quad z = eV/\Delta_\phi. \tag{25}$$

At small voltages, $eV \ll \Delta_\phi$, the magnitude of the shot noise doubles, $P_I = (4/3)eI$, and $C_3 = 4\overline{N}/15$ is four times larger compared to the normal case [8, 2, 27, 1]. When the voltage increases and exceeds the gap edge, $eV > \Delta_\phi$, the normal electron processes at the energies $E > \Delta_\phi$ begin to contribute

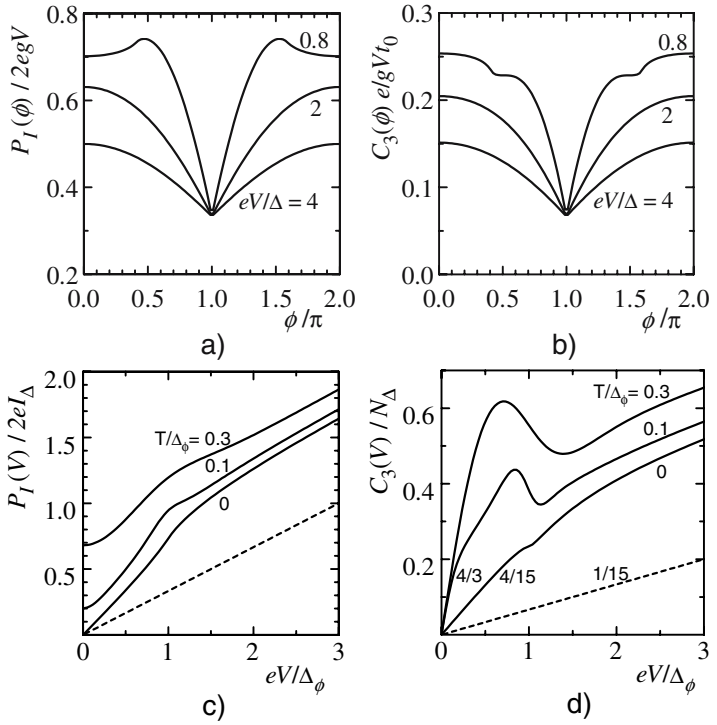

Fig. 2. Shot noise power and third cumulant vs superconducting phase (a, b) at different voltages and $T = 0$, and vs voltage at different temperatures (c, d). Dashed lines denote voltage dependencies in the normal state at $T = 0$. In the panel (d), zero-bias slopes of the normalized $C_3(V)$ are indicated.

to the charge transport, providing the normal-state voltage dependencies of the cumulants at $eV \gg \Delta_\phi$. At large voltage, the Andreev reflected particles produce voltage-independent excess components of the cumulants,

$$I = I_N - I_\Delta f(z) + I^{\rm ex}, \;\; P_I = 2eI_\Delta(z^2-1)f(z) + P_I^{\rm ex}, \;\; I_N = gV, \qquad (26)$$

$$C_3 = \frac{\overline{N}_\Delta}{2}(z+1)\left\{(z-1)\left[8z/3 - (8z^2-3)f(z)\right] - 1/3\right\} + C_3^{\rm ex}, \qquad (27)$$

$$I^{\rm ex} = (I_\Delta/2)\left(\pi^2/4 - 1\right), \;\; P_I^{\rm ex} = 2eI^{\rm ex}, \;\; C_3^{\rm ex} = (\overline{N}_\Delta/2)\left(\pi^2/4 - 4/3\right). \qquad (28)$$

At nonzero temperatures, $T \neq 0$, we calculate the cumulant spectral densities $I(E)$, $P(E)$ and $C(E)$ defined as

$$I = I_\Delta \int_0^\infty dE\, I(E), \;\; P_I = 2eI_\Delta \int_0^\infty dE\, P(E), \;\; C_3 = \overline{N}_\Delta \int_0^\infty dE\, C(E). \qquad (29)$$

Here $I(E) = f_1 \sinh p/Z(0)$, and the functions $P(E)$ and $C(E)$ at $E < \Delta_\phi$ read

$$P(E) = \frac{2}{Z^2(0)} \left[2Qf_1 + (1-f_2)\sinh^2 p\right], \quad Q = 1 + \cosh\epsilon \cosh p, \tag{30}$$

$$C(E) = \frac{\sinh p}{Z^3(0)} \left\{4f_1 \sinh^2\epsilon + (2f_2{+}3f_3)\sinh^2 p + 2Q\left[3(1{-}f_2){-}2f_1\right]\right\}, \tag{31}$$

whereas at $E > \Delta_\phi$ they are given by equations,

$$P(E) = \frac{2}{Z^2(0)}\Big[Q\Big(1 + 2f_1 - 2f_2\frac{\cosh p - 1}{\cosh\epsilon + 1}\Big) + \sinh^2 p - Z(0)\Big], \tag{32}$$

$$\begin{aligned} C(E) = \frac{\sinh p}{Z^3(0)(1+\cosh\epsilon)}\Big\{&4f_1(1+\cosh\epsilon)(Q+\sinh^2\epsilon) \\ &+ 3\big[Z(0)(1-2f_3) + Q\big(4(1-f_2+f_3\cosh\epsilon) + 3\cosh\epsilon - 2f_3\big) \\ &+ \sinh^2\epsilon\big(2f_3 - \cosh\epsilon + (3-5\cosh p)f_2\big)\big] + f_2(5\cosh\epsilon - 1)\sinh^2 p\Big\}, \end{aligned} \tag{33}$$

In Eqs. (30)-(33), the functions

$$f_1 = \theta_\phi \coth\theta_\phi, \quad f_2 = (f_1 - 1)/\sinh^2\theta_\phi, \quad f_3 = (f_2 - 1/3)/\sinh^2\theta_\phi. \tag{34}$$

describe energy variation of quasiparticle spectrum which is most essential in the vicinity of the gap edge Δ_ϕ.

As shown in Fig. 2,(a,b), the cumulants oscillate with the phase and exhibit deep minima at $\phi \bmod 2\pi = \pi$, when the gap closes and the cumulants approach their normal values. When the proximity gap Δ_ϕ approaches eV, $P_I(\phi)$ exhibits a peak, while $C_3(\phi)$ shows a step-like structure. Shown in Fig. 2,(c,d) are voltage dependence of the cumulants for different temperatures plotted as functions of variables that provide the universality of the curves for any ϕ. As the temperature increases, the current noise approaches finite value at $eV = 0$ due to thermal fluctuations, and exhibits quadratic dependence on the applied voltage at $eV \ll T$. Within the intermediate voltage region, $T < eV < \Delta_\phi$, $P_I(V)$ becomes linear with doubled slope produced by the Andreev reflected particles, and at $eV > \Delta_\phi$, the slope turns to its normal-metal value. A considerable excess noise at large voltages is contributed by both the thermal fluctuations and Andreev reflection. A more interesting behavior is discovered for the third cumulant. At nonzero temperature, the zero-bias slope of the normalized $C_3(V)$ is much larger than at zero temperature (up to the factor 5 which is similar to the normal structures [4]), approaching the value 4/3. At larger voltages, $T < eV < \Delta_\phi$, the slope of $C_3(V)$ returns to the value 4/15 found for $T = 0$. At $eV \sim \Delta_\phi$, the curve $C_3(V)$ shows $\mathcal{N}$-like feature, and finally, at $eV > \Delta_\phi$, it approaches a straight line with the (normal-state) slope 1/15. Such a behavior indicates that C_3 acquires anomalously large thermal component at voltage $eV \sim \Delta_\phi$, which, however, rapidly decreases at $eV > \Delta_\phi$ and/or $T > \Delta_\phi$ towards the normal metal level.

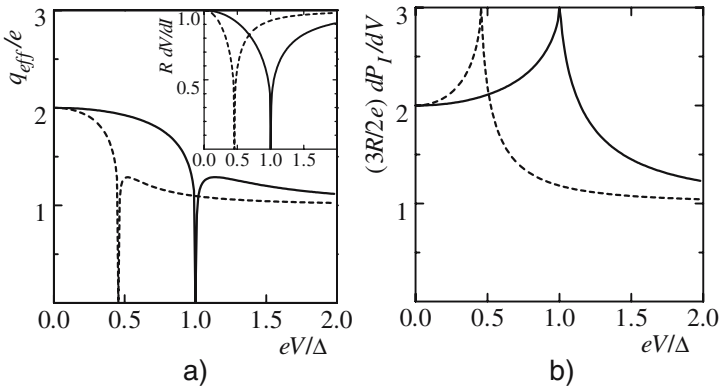

Fig. 3. Effective transferred charge (a), differential noise (b), and differential resistance (inset) vs voltage at $\phi = 0$ (solid lines) and $\phi = 0.7\pi$ (dashed lines), $T = 0$.

The singularity in the DOS at the proximity gap edge produces interesting features of the differential transport characteristics of the interferometer shown in Fig. 3. First, we note that the differential resistance $R_d = dV/dI$ turns to zero at $eV = \Delta_\phi$ (see inset in Fig. 3,a), which is explained by full transmission of the NS junction at the resonant energy Δ_ϕ. Correspondingly, the differential Fano factor $dP_I/dI = R_d(dP_I/dV)$, which is commonly interpreted as effective transferred charge, $q_{eff} = (3/2)dP_I/dI$, also turns to zero, $q_{eff} = 0e$, while the differential noise normalized in a similar way, $(3R/2)$ dP_I/dV, shows a large peak of the height $3e$. Thus we conclude that none of these quantities can be unambiguously associated with the physical elementary transferred charge, but they rather reflect the energy variation of the transmission characteristics. Similar effects have been predicted for an NS structure with opaque interfaces [26] where a considerable enhancement of dP_I/dV and suppression of dP_I/dI occur, however, at small applied voltage determined by large dwell time of quasiparticles.

It is instructive to compare our analytical results for short-arm interferometers with that obtained numerically for long NS junctions with a small minigap $E_g \sim E_{Th} \ll \Delta$. The results are qualitatively similar: in long junctions, q_{eff} is equal to $2e$ at $eV \ll E_g$ and has a minimum at $eV \approx E_g(\phi)$, which moves towards small voltage when at $\phi \to \pi$ [10]; the differential noise is also non-monotonous and approaches maximum at $eV \approx 5E_{Th}$ [9]. After this comparison we see that the proximity gap Δ_ϕ in short junctions plays the role of the minigap E_g in long junctions and determines the feature in the effective charge, though this feature at $eV \sim E_g$ in long junctions is much less pronounced. However, as noted above, a qualitative difference of long junctions is the existence of an intermediate incoherent voltage region $E_g \ll eV \ll \Delta$, where both the effective charge and the normalized differential noise have the value $2e$, and their crossover to e occurs only at $eV \geq \Delta$ [28].

In conclusion, we have studied the full counting statistics of a normal diffusive wire confined between the normal electrode and SNS junction controlled by the magnetic flux through a superconducting loop (Andreev interferometer). Assuming the size of the mesoscopic structure to be much smaller than the coherence length, we calculated analytically the cumulant-generating function for arbitrary applied voltage and temperature. We studied in detail the second (the current noise) and the third cumulants. Both quantities oscillate with the phase difference across the junction and show non-monotonous voltage dependence in the vicinity of the proximity gap edge, which reflects resonant transmission of the structure at the singularity of the density of states.

This work was supported by the U.S. Department of Energy, Office of Science under contract No. W-31-109-ENG-38.

In this Appendix we outline, for reference purposes, the procedure and summarize the results of calculation of the CGF for a diffusive connector between normal reservoirs, by using the extended Keldysh-Green's technique. For generality, we consider a diffusive wire interrupted by tunnel barriers, which enables us to present several original results and to examine various limiting situations.

In normal systems, the matrices $\check{G}$ and $\check{I}$ are traceless in the Keldysh space and therefore they can be expressed through 3-vectors with the components diagonal in the Nambu space, $\check{G} = \boldsymbol{g}\boldsymbol{\tau}$, $\check{I} = \boldsymbol{I}\boldsymbol{\tau}$, where $\boldsymbol{\tau}$ is the vector of the matrices τ, and $\boldsymbol{g}^2 = 1$. Since the lhs of Eq. (4) turns to zero in normal systems, the formal solution of Eq. (4) for the matrix current density $\check{I}_N$ in each segment of the wire can be easily obtained,

$$\begin{aligned} \check{I}_N &= g_N \ln \check{G}_1 \check{G}_2 = g_N \ln[\boldsymbol{g}_1\boldsymbol{g}_2 + i\boldsymbol{\tau}(\boldsymbol{g}_1 \times \boldsymbol{g}_2)] = \boldsymbol{\tau}\boldsymbol{I}_N, \\ \boldsymbol{I}_N &= i g_N \boldsymbol{p}\phi_N, \quad \phi_N = \arccos \boldsymbol{g}_1\boldsymbol{g}_2, \end{aligned} \tag{35}$$

where g_N is the conductivity of the wire segment, $\check{G}_{1,2}$ are the Green's functions at the left and right segment edges, respectively, ϕ_N is the angle between the (complex) unit vectors $\boldsymbol{g}_1$ and $\boldsymbol{g}_2$, and $\boldsymbol{p} = (\boldsymbol{g}_L \times \boldsymbol{g}_R)/\sin\phi_N$ is the unit vector perpendicular to $\boldsymbol{g}_1$ and $\boldsymbol{g}_2$.

The matrix current $\check{I}_B$ through the tunnel barrier can be expressed in terms of Green functions $\check{G}_-$ and $\check{G}_+$ at the left and right sides of the barrier by using the boundary condition [29],

$$\begin{aligned} \check{I}_{B-} = \check{I}_{B+} &= \frac{g_B}{2}[\check{G}_-, \check{G}_+] = \boldsymbol{\tau}\boldsymbol{I}_B, \\ \boldsymbol{I}_B &= i g_B \boldsymbol{p} \sin\phi_B, \quad \phi_B = \arccos \boldsymbol{g}_-\boldsymbol{g}_+, \end{aligned} \tag{36}$$

where $\boldsymbol{p} = (\boldsymbol{g}_- \times \boldsymbol{g}_+)/\sin\phi_B$ and g_B is the barrier conductance.

The conservation of the matrix current along the connector, $\check{I} = \text{const}$, following from Eq. (4) and the boundary condition in Eq. (36), results in conservation of the vector current, $\boldsymbol{I} = \boldsymbol{I}_N = \boldsymbol{I}_B = \text{const}$. This implies that for all elements of the connector, the unit vectors $\boldsymbol{p}$ coincide, therefore the

Green's vectors $\boldsymbol{g}$ lye in plane, and the vector $\boldsymbol{p}$ can be constructed from known Green's vectors $\boldsymbol{g}_L$ and $\boldsymbol{g}_R$ in the reservoirs, $\boldsymbol{p} = (\boldsymbol{g}_L \times \boldsymbol{g}_R)/\sin\phi$, where ϕ is the angle between $\boldsymbol{g}_L$ and $\boldsymbol{g}_R$,

$$\begin{aligned} &\phi = \arccos[1 + P_{-+}(e^{i\chi} - 1) + P_{+-}(e^{-i\chi} - 1)], \\ &P_{\sigma\sigma'} = n_\sigma(1 - n_{\sigma'}), \;\; n_- = n_F(E), \; n_+ = n_F(E + eV). \end{aligned} \tag{37}$$

From the current conservation, we also conclude that all elements are characterized by a single variable η,

$$g_B \sin\phi_B = g_N \phi_N = g\eta = \text{ const}, \tag{38}$$

where the normalization constant g is chosen to be equal to the conductance of the whole connector. Thus, the vector current is given by equation,

$$\boldsymbol{I} = \frac{ig\eta}{\sin\phi}(\boldsymbol{g}_L \times \boldsymbol{g}_R). \tag{39}$$

The planar rotation of the Green's vector results in the additivity of the angles between all consecutive vectors $\boldsymbol{g}$, therefore the sum of these angles is equal to ϕ,

$$\sum_{wires} \phi_N + \sum_{barriers} \phi_B = \phi = \arccos(\boldsymbol{g}_L \boldsymbol{g}_R), \tag{40}$$

which leads to the equation for the parameter $\eta(\phi)$,

$$\gamma_N \eta + \sum\nolimits_k \arcsin(\gamma_k \eta) = \phi, \quad \gamma_N = R_N/R, \quad \gamma_k = R_k/R, \quad \gamma_N + \sum\nolimits_k \gamma_k = 1, \tag{41}$$

where R_N is the net resistance of all wires, R_k is the resistance of the k-th barrier, and $R = g^{-1}$.

By using the definitions in Eq. (3), we obtain the counting electric current $I(\chi)$ and the CGF,

$$I(\chi) = \frac{1}{2e}\int_0^\infty dE \mathrm{Tr}\sigma_z \boldsymbol{I}_x = \frac{ig}{2e}\int_0^\infty dE \mathrm{Tr}\frac{\sigma_z \eta}{\sin\phi}(\boldsymbol{g}_L \times \boldsymbol{g}_R)_x, \tag{42}$$

$$S(\chi) = \frac{gt_0}{4e^2}\int dE \mathrm{Tr}\Big[r_N\eta^2/2 + \sum\nolimits_k \Big(1 - \sqrt{1 - r_k^2\eta^2}\Big)/r_k\Big], \tag{43}$$

We note that the statistics is insensitive to the position of the barriers and depends only on the barrier resistances and the net resistance of the diffusive part of the connector. In the absence of barriers, $r_k \to 0$, the CGF reads

$$\begin{aligned} S(\chi) &= \frac{gt_0}{4e^2}\int dE\, \phi^2 \\ &= \frac{gt_0}{4e^2}\int dE\, \arccos^2\Big[1 + P_{-+}\Big(e^{i\chi} - 1\Big) + P_{+-}\Big(e^{-i\chi} - 1\Big)\Big]. \end{aligned} \tag{44}$$

At zero temperature, the integration over energy in Eq. (43) can be explicitly performed,

$$S(\chi) = \frac{\overline{N}}{2}\Big[r_N\eta^2/2 + \sum\nolimits_k \Big(1 - \sqrt{1 - r_k^2\eta^2}\Big)/r_k\Big], \tag{45}$$

where $\overline{N} = gVt_0/e$. From Eq. (45) we find the Fano factor F in the shot noise power $P_I = eFI$,

$$F = (2/3)\,(1 + 2B_3)\,, \qquad B_n = \sum\nolimits_k r_k^n, \tag{46}$$

which varies between the Poissonian value $F = 2$ for the tunnel connector and 1/3-suppressed value, $F = 2/3$, in the absence of barriers. The third cumulant C_3 varies between $\overline{N}$ for Poissonian statistics in the single barrier case and $\overline{N}/15$ for a diffusive conductor,

$$C_3(V, 0) = \big(\overline{N}/15\big)\,[1 + 10B_3\,(1 + 4B_3) - 36B_5]\,. \tag{47}$$

It is interesting to note that Eq. (41) can be easily transformed into equation for the transparency distribution $\rho(\mathrm{T})$, by making use of the relation of the generalized circuit theory between the counting current $I(\chi)$ and the matrix current $\check{I}$ following from Eqs. (6) and (3),

$$I(\chi) = \frac{1}{4e}\int_0^\infty dE\mathrm{Tr}\tau_x\sigma_z\check{I}, \quad \check{I} = \frac{g}{2}\int_0^1 d\mathrm{T}\rho(\mathrm{T})\mathrm{T}[\check{G}_L, \check{G}_R(\chi)]\check{W}^{-1}. \tag{48}$$

Rewriting these equations in the vector representation, comparing them with Eq. (42), and introducing the variable $z = (1 - \boldsymbol{g_L g_R})/2$, we obtain the equation for $\rho(\mathrm{T})$,

$$\int_0^1 \frac{\mathrm{T}d\mathrm{T}\rho(\mathrm{T})}{1 - z\mathrm{T}} = \frac{\eta}{2\sqrt{z(1-z)}}, \tag{49}$$

where η obeys Eq. (41) with the function $\phi(z) = 2\arcsin\sqrt{z}$ in the right-hand side (rhs). The solution of Eq. (49) has the form $\rho(\mathrm{T}) = \mathrm{Re}\,\eta/2\pi\mathrm{T}\sqrt{1-\mathrm{T}}$, where $\eta(\mathrm{T})$ is the solution of Eq. (41) with the function $\pi + 2i\,\mathrm{arccosh}(1/\sqrt{\mathrm{T}})$ in the rhs [24].

In some limiting cases, one can obtain an analytical solution of Eq. (41). In particular, if the number M of the barriers is large, $M \gg 1$, then the resistance of each barrier is small compared to the net resistance, $R_k \ll R$. In this case, the approximate solution of Eq. (41) is $\eta = \phi$, and the CGF coincides with that for diffusive wire, Eq. (44). In the tunnel limit, when the resistance of each barrier much exceeds the net resistance of diffusive segments, $R_k \gg R_N$, the first term in Eq. (41) can be neglected. Then an analytical expression for the parameter η and the CGF at arbitrary M can be obtained in the case of equivalent barriers, $r_k = 1/M$,

$$\eta = M\sin\frac{\phi}{M}, \quad S(\chi) = \overline{N}M^2\sin^2\frac{\arccos e^{i\chi/2}}{M}, \tag{50}$$

when the Fano factor is given by $F = (2/3)\left(1 + 2/M^2\right)$. In the limit of large number of the barriers, $M \gg 1$, we return to the diffusive statistics, while for single-barrier structure, $M = 1$, we obtain Poissonian statistics, $S(\chi) = \overline{N}(e^{i\chi} - 1)$.

At arbitrary temperature, the cumulants can be found analytically by asymptotic expansion in Eqs. (41), (43) over small η and χ. In particular, the noise power,

$$P_I(V,T) = \frac{4T}{3R}\left[(1 + 2B_3)\,\frac{p}{2}\coth\frac{p}{2} + 2(1 - B_3)\right], \tag{51}$$

exhibits crossover between the shot noise at $T \ll eV$ and the Johnson thermal noise $P_T = 4T/R$ at large temperature, $T \gg eV$. The voltage dependence of the third cumulant,

$$C_3(V,T) = C_3(V,0) + \frac{2}{5}\overline{N}(1 - 10B_3^2 + 9B_5)\frac{\sinh p - p}{p\sinh^2(p/2)}, \tag{52}$$

is linear in both limits and approaches $(\overline{N}/3)(1 + 2B_3)$ at high temperatures. In the absence of barriers, $B_n = 0$, Eq. (52) reproduces the result of a modified kinetic theory of fluctuations for a diffusive wire [4].

In order to access FCS in multi-terminal structures, which consist of a set of connectors attached between several normal electrodes and a diffusive island (node) with negligibly small resistance, separate counting fields χ_α and parameters η_α are to be introduced in each arm [16],

$$\boldsymbol{I}_\alpha = i\xi_\alpha(\boldsymbol{g}_\alpha \times \boldsymbol{g}_c), \qquad \xi_\alpha = g_\alpha\eta_\alpha/\sin\phi_\alpha. \tag{53}$$

The quantities η_α obey the equations similar to Eq. (41), with the angles $\phi_\alpha = \arccos(\boldsymbol{g}_\alpha\boldsymbol{g}_c)$ in the rhs, where the Green's vector $\boldsymbol{g}_c$ at the node can be found from the current conservation law, $\sum_\alpha \boldsymbol{I}_\alpha = 0$,

$$\boldsymbol{g}_c = \boldsymbol{G}/\sqrt{\boldsymbol{G}^2}, \quad \boldsymbol{G} = \sum\nolimits_\alpha \xi_\alpha \boldsymbol{g}_\alpha. \tag{54}$$

According to Eq. (54), the vector $\boldsymbol{g}_c$ depends on all counting fields χ_α, which reflects cross-correlations between the currents in different connectors. For the system of tunnel connectors, where the quantities ξ_α are equal to the conductances g_α and therefore become independent of χ, the CGF at zero temperature can be explicitly evaluated [21],

$$S\{\chi\} = \frac{Vt_0}{2e}G\sqrt{1 + 4\sum\nolimits_\alpha \overline{g}_V\overline{g}_\alpha(e^{i\chi_\alpha} - 1)}, \quad \overline{g}_\alpha = g_\alpha/G, \quad G = \sum\nolimits_\beta g_\beta, \tag{55}$$

where the index V denotes the voltage biased electrode.

For arbitrary connectors, the cumulants can be found from asymptotic solutions of the equations for η_α and $\boldsymbol{g}_c$ at small χ_α. For instance, the partial

current through α-th connector is $I_\alpha = V g_\alpha \overline{g}_V$, and the Fano factors defined as $F_{\alpha\beta} = (2ei/I_\alpha)(\partial I_\alpha\{\chi\}/\partial\chi_\beta)_{\chi=0}$ read

$$F_{\alpha\beta} = \Big(2-\frac{4}{3}\overline{g}_V\Big)\delta_{\alpha\beta} - \frac{4}{3}\overline{g}_\beta\Big[1+\overline{g}_V(B_{3\alpha}+B_{3\beta}) - B_{3V}(1-\overline{g}_V)^2 - \overline{g}_V\sum_{\gamma\neq V}\overline{g}_\gamma B_{3\gamma}\Big]. \tag{56}$$

The diagonal elements $F_{\alpha\alpha}$ of the matrix $F_{\alpha\beta}$ have the meaning of the Fano factors for the shot noise in α-th connector and may vary between 2/3 and 2. For large number of the terminals, when the normalized conductances $\overline{g}_\alpha$ become small, they approach Poissonian value $F_{\alpha\alpha} = 2$. The cross-correlators $F_{\alpha\beta}$ ($\alpha \neq \beta$) between the currents in different terminals are negative due to Pauli principle [28]. In a particular case of diffusive connectors ($B_\alpha = 0$), Eq. (56) reproduces the result of Ref. [30] for a so-called star-shaped geometry.

References

1. L.S. Levitov and G.B. Lesovik, JETP Lett. **58**, 230 (1993); H. Lee, L.S. Levitov, and A.Yu. Yakovets, Phys. Rev. B **51**, 4079 (1995); L.S. Levitov, H.W. Lee, and G.B. Lesovik, J. Math. Phys. **37**, 4845 (1996).
2. B.A. Muzykantskii and D.E. Khmelnitskii, Physica B **203**, 233 (1994).
3. Ya.M. Blanter and M. Büttiker, Phys. Rep. **336**, 1 (2000).
4. K.E. Nagaev, Phys. Rev. B **66**, 075334 (2002); D.B. Gutman and Yu. Gefen, *ibid.* **68**, 035302 (2003).
5. B. Reulet, J. Senzier, and D.E. Prober, cond-mat/0302084, Phs. Rev. Lett. **91**, 196601 (2003).
6. C.W.J. Beenakker, M. Kindermann, and Yu.V. Nazarov, Phys. Rev. Lett. **90**, 176802 (2003).
7. A.F. Andreev, Sov. Phys. JETP **19**, 1228 (1964).
8. V.A. Khlus, Sov. Phys. JETP **66**, 1243 (1987); M.J.M. de Jong and C.W.J. Beenakker, Phys. Rev. B **49**, 16070 (1994).
9. W. Belzig and Yu.V. Nazarov, Phys. Rev. Lett. **87**, 067006 (2001); M.P.V. Steinberg and T.T. Heikkilä, Phys. Rev. B **66**, 144504 (2002).
10. B. Reulet, A.A. Kozhevnikov, D.E. Prober, W. Belzig, and Yu.V. Nazarov, Phys. Rev. Lett. **90**, 066601 (2003).
11. C.J. Lambert and R. Raimondi, J. Phys.: Condens. Matter **10**, 901 (1998).
12. F.W.J. Hekking and Yu.V. Nazarov, Phys. Rev. Lett. **71**, 1625 (1993); H. Nakano and H. Takayanagi, Phys. Rev. B **47**, 7986 (1993).
13. Yu.V. Nazarov, Ann. Phys. (Leipzig) **8**, SI-193 (1999).
14. W. Belzig, in *Quantum Noise in Mesoscopic Physics*, ed. by Yu.V. Nazarov, NATO Science Series **97**, 463 (2003).
15. A.I. Larkin, and Yu.N. Ovchinnikov, Sov. Phys. JETP **41**, 960 (1975); **46**, 155 (1977).
16. Yu.V. Nazarov and D.A. Bagrets, Phys. Rev. Lett. **88**, 196801 (2002).
17. T.T. Heikkilä, J. Särkkä, and F.K. Wilhelm, Phys. Rev. B **66**, 184513 (2002); E.V. Bezuglyi, V.S. Shumeiko, and G. Wendin, *ibid.* **68**, 134506 (2003).
18. I.O. Kulik and A.N. Omelyanchouk, JETP Lett. **21**, 96 (1975).

19. Yu.V. Nazarov, Superlatt. Microstruct. **25**, 1221 (1999).
20. W. Belzig and Yu.V. Nazarov, Phys. Rev. Lett. **87**, 197006 (2001).
21. J. Börlin, W. Belzig, and C. Bruder, Phys. Rev. Lett. **88**, 197001 (2002).
22. J.C. Cuevas and W. Belzig, Phys. Rev. Lett. **91**, 187001 (2003); G. Johansson, P. Samuelsson, and Å. Ingerman, Phys. Rev. Lett. **91**, 187002 (2003).
23. O.N. Dorokhov, JETP Lett. **36**, 318 (1982); Solid State Comm. **51**, 381 (1984); P.A. Mello, P. Pereyra, and N. Kumar, Ann. Phys. **181**, 290 (1988).
24. Yu.V. Nazarov, Phys. Rev. Lett. **73**, 136 (1994); W. Belzig, A. Brataas, Yu.V. Nazarov, and G.E.W. Bauer, Phys. Rev. B **62**, 9726 (2000).
25. W. Belzig and P. Samuelsson, Europhys. Lett. **64**, 253 (2003).
26. P. Samuelsson, Phys. Rev. B **67**, 054508 (2003).
27. K.E. Nagaev, Phys. Lett. A **169**, 103 (1992); C.W.J. Beenakker and M. Büttiker, Phys. Rev. B **46**, 1889 (1992).
28. K.E. Nagaev and M. Büttiker, Phys. Rev. B **63**, 081301 (2001).
29. M.Yu. Kupriyanov and V.F. Lukichev, Sov. Phys. JETP **67**, 89 (1988).
30. E.V. Sukhorukov and D. Loss, Phys. Rev. Lett. **80**, 4959 (1998); Phys. Rev. B **59**, 13054 (1999).